Hyperfine Interact (2016) 237:44
DOI 10.1007/s10751-016-1278-5

^{57}Fe Mössbauer spectroscopic studies of single-crystalline $K_xFe_{2-y}S_2$ and $K_xFe_{2-y}Se_2$

Yuu Tsuchiya[1] · Shugo Ikeda[1] · Hisao Kobayashi[1]

Abstract We have investigated the physical properties of single-crystalline $K_xFe_{2-y}S_2$ and $K_xFe_{2-y}Se_2$ samples using ^{57}Fe Mössbauer spectroscopy. The observed ^{57}Fe Mössbauer spectra were reconstructed using a major antiferromagnetic ordered $K_2Fe_4Se_5$ phase and a minor paramagnetic phase down to 5 K, despite being superconducting below 32.2 K in $K_xFe_{2-y}Se_2$. The analysis of ^{57}Fe Mössbauer spectrum for $K_xFe_{2-y}S_2$ at 290 K confirms the presence of a major antiferromagnetic ordered $K_2Fe_4S_5$ phase and a minor paramagnetic phase in the $K_xFe_{2-y}S_2$ single crystal. The derived hyperfine interaction parameters of the paramagnetic phase in $K_xFe_{2-y}S_2$ suggest that the microstructure of this phase in $K_xFe_{2-y}S_2$ is similar to that of the superconducting phase in $K_xFe_{2-y}Se_2$ although the $K_xFe_{2-y}S_2$ single crystals exhibit no superconductivity down to 5 K.

Keywords Iron-based superconductor · Phase separation · Mössbauer spectroscopy

1 Introduction

The newly discovered alkaline iron selenide superconductors $K_xFe_{2-y}Se_2$, with superconducting transition temperatures (T_c) around 32 K at ambient pressure contain two distinct phases in their microstructures by a phase separation [1–3]. One is a major insulating phase with a chemical formula $K_2Fe_4Se_5$ and the other is a minor superconducting phase. The structures of these two phases are related to the tetragonal $ThCr_2Si_2$ structure with the $I4/mmm$ space group. In the major insulating phase, Fe vacancies in FeSe layers are ordered

This article is part of the Topical Collection on *Proceedings of the International Conference on the Applications of the Mössbauer Effect (ICAME 2015), Hamburg, Germany, 13–18 September 2015*

✉ Yuu Tsuchiya
tsuchiya.yuu1990@gmail.com

[1] University of Hyogo, 3-2-1 Koto, Ako, Hyogo 678-1297, Japan

Published online: 22 February 2016

in the *ab* plane, which is characterized by a modulation of $q_1 = 1/5$ (3a*+b*), where $a*$ and $b*$ represent the reciprocal lattice parameters a and b in the tetragonal $ThCr_2Si_2$ structure. An antiferromagnetic (AFM) transition occurs at $T_N = 559$ K in the major insulating phase and its magnetic structure was determined to be a collinear AFM one with $Q_m = (101)$ by neutron diffraction [4], where the magnetic easy axis is along the c-axis and the Fe magnetic moment was evaluated to be $\sim 3.3\ \mu_B$. In the minority superconducting phase, the structure is characterized by a modulation of $q_2 = 1/2(a* + b*)$ originating from the K-vacancy order in the *ab* plane [3]. The phaseseparated pattern on the micrometer scale often adopts notable stripe configurations along the <110> direction in the *ab* plane and these stripe areas correspond to the superconducting phase [2, 3]. The area ratio between the insulating and the superconducting phases was estimated to be about 4:1 [2, 5].

The scanning and transmission electron microscopic studies reveal also a phase separation in $K_xFe_{2-y}S_2$, where the microstructures depend on the Fe concentrations [6]. In $K_{0.8}Fe_{1.8}S_2$ the two microstructures are similar to those in the $K_xFe_{2-y}Se_2$ superconductors [6]. In $K_{0.8}Fe_{1.55}S_2$, however, two microstructures are characterized by two different Fe-vacancy orders with $q_1 = 1/5(3a* + b*)$ and $q_3 = 1/4(3a* + b*)$, respectively [6]. The X-ray diffraction studies indicate that $K_{0.88}Fe_{1.63}S_2$ has the $I4/m$ symmetry, incorporating the Fe-vacancy order site as in the case of the AFM ordered $K_2Fe_4Se_5$ phase [7]. From the results of the magnetization measurements, $K_xFe_{2-y}S_2$ with a similar composition to the $K_xFe_{2-y}Se_2$ superconductors shows an AFM transition at $T_N = 565$ K [8] with spin-glass-like behavior and no superconductivity below 32 K [7, 8] The systematic investigations of the electronic states of the Fe atoms in $K_xFe_{2-y}Ch_2$ (Ch = S and Se) are important for understanding the mechanism of superconductivity in $K_xFe_{2-y}Se_2$.

We have synthesized the single-crystalline $K_xFe_{2-y}Ch_2$ and measured the ^{57}Fe Mössbauer spectra of $K_xFe_{2-y}Ch_2$ using the single crystals to investigate the microstructures and the electronic states of the Fe atoms in $K_xFe_{2-y}Ch_2$.

2 Experimental details

Single crystals of $K_xFe_{2-y}Ch_2$ were grown by a self-flux method [8, 9] The polycrystalline FeS starting materials were synthesized from stoichiometric mixtures of Fe chunks (4N) and S chunks (6N) by gradually heating up to 800 °C for 12 h. The polycrystalline FeSe starting materials were also synthesized from stoichiometric mixtures of Fe chunks (4N) and Se chunks (4N) by gradually heating up to 1000 °C for 12 h. The K pieces and the FeCh polycrystals were sealed into two wall quartz tubes with the nominal composition K:FeCh = 0.8:2 with argon gas under a pressure of 0.4 atmospheres at room temperature. These mixtures were heated to 1050 °C in 4 h and then kept at 1050 °C for 2 h, and later slowly cooled down to 750 °C at a rate of 6 °C/h. After that, the mixtures were cooled down to room temperature by shutting down the furnace. The plate-like $K_xFe_{2-y}Ch_2$ single crystals were cleaved from the final products. The typical dimensions of the obtained plate-like single crystals are $\sim 3 \times 3 \times 1\ mm^3$.

X-ray diffraction pattern were measured with Cu K_α radiation using a Rigaku Miniflex II diffractometer equipped with a graphite crystal monochromator for removal of the Cu K_β radiation and fluorescence X-rays from the sample. The magnetization measurements were carried out by using a Quantum Design MPMS-SQUID magnetometer. The ^{57}Fe Mössbauer experiments were performed using a conventional constant-acceleration type spectrometer with a ^{57}Co in Rh source and the velocity scale was calibrated with an α-Fe foil. The

absorbers with an area of 80 mm^2 were composed of the several plate-like $K_xFe_{2-y}Ch_2$ single crystals with the tetragonal c-axis perpendicular the absorber planes. The thicknesses of the $K_xFe_{2-y}Se_2$ and $K_xFe_{2-y}S_2$ absorbers are approximately 40 and 100 μm, respectively. The direction of the incident γ-rays was parallel to the tetragonal c-axis of the $K_xFe_{2-y}Ch_2$ absorber.

3 Results and discussion

All sharp diffraction peaks in the X-ray diffraction patterns observed in the $K_xFe_{2-y}Ch_2$ single crystals are indexed by the (00l) diffraction, indicating that the crystallographic c-axes are perpendicular to the surfaces of the plate-like single crystals. The lattice constant of the c-axis for $K_xFe_{2-y}Se_2$ was evaluated to be 14.13(6) Å from the (00l) diffraction peaks by extrapolating the apparent lattice constant to zero ($\theta = 90°$) of the Nelson-Riley function. This value is comparable with those of the previous reports [1, 5, 9, 10]. The diffraction peaks are attributed to the AFM ordered $K_2Fe_4Se_5$ phase with the $I4/m$ space group. The lattice constant of the c-axis for $K_xFe_{2-y}S_2$ was evaluated to be 13.53(4) Å by the same procedure as for $K_xFe_{2-y}Se_2$, which is consistent with those of $K_2Fe_4S_5$ within our experimental error [7, 8].

Figure 1 shows the external magnetic field, H, dependence of the magnetization, M, for the $K_xFe_{2-y}S_2$ single crystal at 5 K with H perpendicular to the c-axis. Since M of $K_xFe_{2-y}S_2$ almost linearly increases with H, $K_xFe_{2-y}S_2$ is in a normal conducting state down to 5 K and the magnetic susceptibility was evaluated to be 2.1×10^{-3} emu/mol at 5 K which is quantitatively consistent with the previous reports [7, 8]. In contrast superconductivity appears below $T_c^{onset} = 32.2$ K in the single-crystalline $K_xFe_{2-y}Se_2$ samples, which was determined from the temperature dependence of M for $K_xFe_{2-y}Se_2$ with $H = 10$ Oe. This T_c^{onset} value is in good agreement with those of the previous reports [1–5, 9]. The M

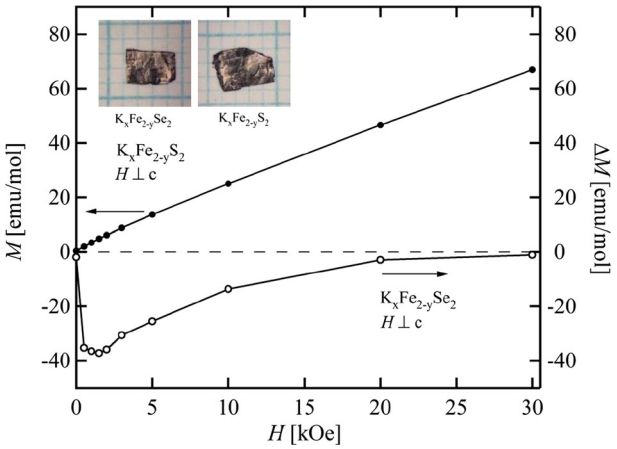

Fig. 1 Magnetic field, H, dependence of the magnetization, M, for the $K_xFe_{2-y}S_2$ single crystal (*solid circles*) and the magnetization, ΔM, of the superconducting phase for the $K_xFe_{2-y}Se_2$ single crystal (*open circles*) at 5 K with H perpendicular to the c-axis. The ΔM values were evaluated from the difference between the M values at 5 K and above T_c^{onset} for the $K_xFe_{2-y}Se_2$ single crystal

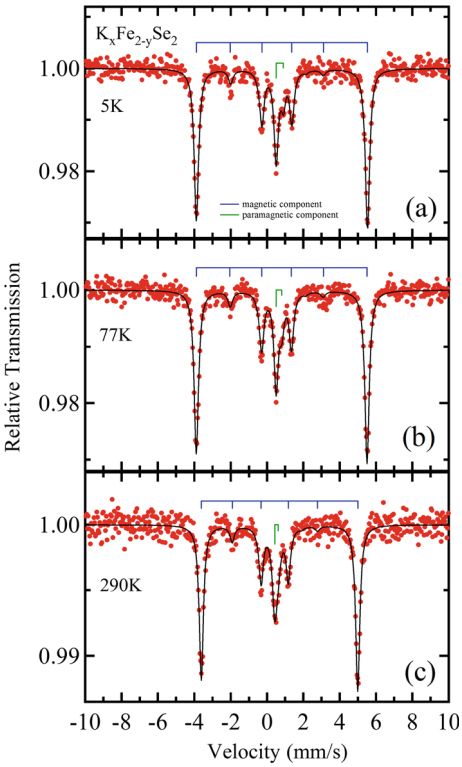

Fig. 2 ^{57}Fe Mössbauer spectra of the singlecrystalline $K_xFe_{2-y}Se_2$ absorber observed at **a** 5 K, **b** 77 K, and **c** 290 K. The *red circles* and the *solid lines* indicate the observed spectra and the results of the fittings, respectively. The bar spectra represent two extracted components in each spectrum [5, 11]

values with $H = 10$ kOe are almost independent of temperature from T_c^{onset} to 300 K. The AFM ordered $K_2Fe_4Se_5$ and the superconducting phases coexist in the $K_xFe_{2-y}Se_2$ single crystal. Since the superconducting phase is in the Pauli paramagnetic state above T_c^{onset}, the M values above T_c^{onset} for $K_xFe_{2-y}Se_2$ mainly originate from the AFM ordered $K_2Fe_4Se_5$ phase. Thus, we have evaluated the magnetization, ΔM, at 5 K for the superconducting phase in the $K_xFe_{2-y}Se_2$ single crystal from the difference between the M values at 5 K and above T_c^{onset}. As seen in Fig. 1, $K_xFe_{2-y}Se_2$ shows diamagnetism up to $H = 30$ kOe and the shape of ΔM is similar to that of a typical type-II superconductor.

The ^{57}Fe Mössbauer spectra observed using the single-crystalline $K_xFe_{2-y}Se_2$ absorber are shown in Fig. 2. The spectrum at 5 K consists of a major magnetic sextet and a minor paramagnetic doublet. As seen in Fig. 2, these characteristic features in the spectra do not change with increasing temperature to 290 K. The minor paramagnetic doublet is asymmetry and the intensity ratio is almost 3:1, indicating that the z-axis of the diagonalized electric-field-gradient tensor at the paramagnetic Fe site is parallel to the c-axis of the crystal. We have analyzed these Mössbauer spectra according to the procedures given by Z. Li et al. [5] and V. Ksenofontov et al. [11], where the ^{57}Fe nuclear Hamiltonian for the magnetic and the electric quadrupole interactions with arbitrary relative orientation was diagonalized within the assumption of the asymmetry parameter $\eta\ (= (V_{xx} - V_{yy})/V_{zz}) =$ for the major magnetic sextet. As shown in Fig. 2, all observed spectra were reconstructed using the major magnetic sextet (79 %) and the minor paramagnetic doublet (21 %). The derived hyperfine interaction parameters are listed in Table 1. The corresponding parameters derived from the major magnetic sextet in the spectrum at 5 K are in good agreement with those obtained

Table 1 Derived center shift, δ_{cs}, electric quadrupole interaction, $eQV_{zz}/2$, magnetic hyperfine field, H_{hf}, and angle, θ, between the z-axis of the diagonalized electric field gradient tensor and the direction of H_{hf} for $K_xFe_{2-y}Se_2$ and $K_xFe_{2-y}S_2$

		δ_{cs} (mm/s)	$eQV_{zz}/2$(mm/s)	H_{hf} (kOe)	θ (°)
$K_xFe_{2-y}Se_2$					
5 K	Mag.	0.68(1)	1.14(2)	285.5(5)	44(3)
	Paramag.	0.70(2)	−0.40(2)		
77 K	Mag.	0.67(2)	1.08(3)	284.0(5)	43(4)
	Paramag.	0.66(3)	−0.314(2)		
290 K	Mag.	0.56(2)	0.96(3)	260.7(7)	43(5)
	Paramag.	0.52(3)	−0.19(3)		
$K_xFe_{2-y}S_2$					
290 K	Mag.	0.54(1)	1.00(2)	267.4(3)	47(2)
	Paramag.	0.49(1)	−0.20(2)		

from the spectra at 10 K [5, 11]. The evaluated intensity ratio between the major magnetic sextet and the minor paramagnetic doublet is qualitatively consistent with the area ratio between the AFM ordered $K_2Fe_4Se_5$ and the superconducting (stripe patterns area) phases, which was estimated by the scanning electron microscopic study [2]. Accordingly, the major magnetic sextet in the observed spectra results from the Fe atoms at the 16*i* site in the AFM ordered $K_2Fe_4Se_5$ phase with the $I4/m$ space group and the minor paramagnetic doublet is attributed to the Fe atoms in the superconducting phase.

Figure 3 shows the ^{57}Fe Mössbauer spectrum of the single-crystalline $K_xFe_{2-y}S_2$ absorber at 290 K. As seen in this figure and Fig. 2c, the characteristic features are similar to those of the single-crystalline $K_xFe_{2-y}Se_2$ absorber at 290 K Therefore we have also analyzed the Mössbauer spectrum of $K_xFe_{2-y}S_2$ using the same procedure as for $K_xFe_{2-y}Se_2$. The spectrum was well fitted using a major magnetic sextet (88 %) and a minor paramagnetic doublet (12 %). The derived hyperfine interaction parameters are listed in Table 1. The hyperfine interaction parameters of the major magnetic sextet are comparable with those for $K_xFe_{2-y}Se_2$ at 290 K. The results indicate that the Fe electronic state in the major magnetic sextet of $K_xFe_{2-y}S_2$ is similar to that in the AFM ordered $K_2Fe_4Se_5$ phase. The superlattice diffraction peaks were observed in $K_{0.88}Fe_{1.63}S_2$ by the X-ray diffraction, indicating that the crystal structure of $K_{0.88}Fe_{1.63}S_2$ has the $I4/m$ symmetry [7]. Therefore, the major magnetic sextet of the $K_xFe_{2-y}S_2$ spectrum results from the Fe atoms at the 16*i* site of the AFM ordered $K_2Fe_4S_5$ phase.

The intensity ratio in the paramagnetic doublet extracted from the Mössbauer spectrum of $K_xFe_{2-y}S_2$ indicates again that the z-axis of the diagonalized electricfield-gradient tensor at the paramagnetic Fe site is parallel to the crystalline c-axis. As seen in Table 1, the derived $eQV_{zz}/2$ value agrees with that of the paramagnetic Fe site in $K_xFe_{2-y}Se_2$ at 290 K within our experimental error. These results suggest that the local symmetry at the paramagnetic Fe site in $K_xFe_{2-y}S_2$ is very similar to that at the paramagnetic Fe site of the superconducting phase in $K_xFe_{2-y}Se_2$. Furthermore, the derived δ_{cs} value is consistent with that of the paramagnetic Fe site in $K_xFe_{2-y}Se_2$ at 290 K. Thus, the microstructure of the paramagnetic component in $K_xFe_{2-y}S_2$ is similar to that of the superconducting phase in $K_xFe_{2-y}Se_2$. However, the $K_xFe_{2-y}S_2$ single crystals do not exhibit superconductivity down to 5 K. Since the evaluated c-lattice parameter of $K_xFe_{2-y}S_2$ is about 5 % shorter

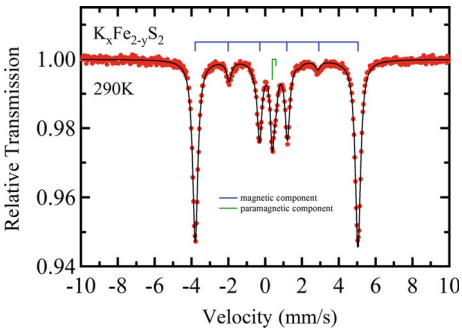

Fig. 3 ^{57}Fe Mössbauer spectrum of the singlecrystalline $K_xFe_{2-y}S_2$ absorber observed at 290 K. The *red circles* and the *solid line* indicate the observed spectrum and the result of the fitting, respectively. The bar spectra represent two extracted components in the spectrum [5, 11]

than that of $K_xFe_{2-y}Se_2$, the local volume of the FeS_4 tetrahedron is smaller than that of the $FeSe_4$ tetrahedron. Generally, Fe-S bonds are more covalent than Fe-Se bonds. The smaller local volume and the covalent character in the Fe-S bonds may affect the Fe electronic state in the paramagnetic component in $K_xFe_{2-y}S_2$. Although δ_{cs} is a good scale for the Fe electronic state, there are two different components contributing to δ_{cs}. One is the isomer shift which is directly related to a Fe electronic state in a compound and the other is the second-order Doppler shift which comes from vibrational properties of Fe atoms in a compound and on the local binding strength, as expressed by the local Debye temperature. The contribution of the second-order Doppler shift to δ_{cs} can be determined by measuring the temperature dependence of δ_{cs} as demonstrated recently for related FeSe-based superconductors [12]. Therefore, we plan to measure Mössbauer spectra of the single-crystalline $K_xFe_{2-y}S_2$ absorber at low temperatures to investigate the Fe electronic states of the two microstructures in $K_xFe_{2-y}S_2$.

Finally, we have to mention that the exact compositions of our single-crystalline $K_xFe_{2-y}Ch_2$ samples have not been determined so far directly. In our single-crystalline $K_xFe_{2-y}Se_2$ samples, however, the *c*-lattice parameter evaluated and the results of the magnetization and ^{57}Fe Mössbauer measurements suggest that the composition is very near to that of the $K_{0.8}Fe_{1.99}Se_2$ superconductors [5]. From the evaluated values of the *c*-lattice parameter and the magnetic susceptibility, our single-crystalline $K_xFe_{2-y}S_2$ samples may have a similar composition to that of the $K_{0.88}Fe_{1.63}S_2$ compound [7].

4 Summary

The $K_xFe_{2-y}Ch_2$ single crystals were synthesized by the self-flux method. We have measured the ^{57}Fe Mössbauer spectra of the $K_xFe_{2-y}Ch_2$ single-crystalline samples. Despite being superconducting below $T_c^{onset} = 32.2$ K, all observed ^{57}Fe Mössbauer spectra of the single-crystalline $K_xFe_{2-y}Se_2$ absorber were reconstructed using the major AFM ordered $K_2Fe_4Se_5$ phase and the minor paramagnetic superconducting phase in the temperature range from 5 to 290 K. ^{57}Fe Mössbauer study of the $K_xFe_{2-y}S_2$ single crystals at 290 K confirms the presence of the major AFM ordered $K_2Fe_4S_5$ phase and the minor paramagnetic phase. The derived δ_{cs} and $eQV_{zz}/2$ values of the paramagnetic phase in the $K_xFe_{2-y}S_2$ single crystal indicate that the microstructure of the paramagnetic phase in $K_xFe_{2-y}S_2$ is similar to that of the superconducting phase in $K_xFe_{2-y}Se_2$ although the $K_xFe_{2-y}S_2$ single crystals do not exhibit superconductivity.

Acknowledgments One of us (Y.T.) was financially supported by the Research Foundation for the Electrotechnology of Chubu (REFEC), No. E-27119.

References

1. Guo, J., Jin, S., Wang, G., Wang, S., Zhu, K., Zhou, T., He, M., Chen, X.: Superconductivity in the iron selenide $K_xFe_{2-y}Se_2$ ($0 \leq x \leq 1.0$). Phys. Rev. B **82**, 180520 (2010)
2. Ding, X., Fang, D., Wang, Z., Yang, H., Liu, J., Deng, Q., Ma, G., Meng, C., Hu, Y., Wen, H.H.: Influence of microstructure on superconductivity in $K_xFe_{2y}Se_2$ and evidence for a new parent phase $K_2Fe_7Se_8$. Nat. Commun. **4**, 1897 (2012)
3. Wang, Z.W., Wang, Z., Song, Y.J., Ma, C., Cai, Y., Chen, Z., Tian, H.F., Yang, H.X., Chen, G.Fu., Li, J.Q.: Structural phase separation in $K_{0.8}Fe_{1.6+x}Se_2$ superconductors. J. Phys. Chem. C **116**, 17847–17852 (2012)
4. Bao, W., Huang, Q.Z., Chen, G.F., Green, M.A., Wang, D.M., He, J.B., Qiu, Y.M.: A novel large moment antiferromagnetic order in $K_{0.8}Fe_{16}Se_2$ superconductor. Chin Phys. Lett. **28**, 086104 (2011)
5. Li, Z., Ma, X., Pang, H., Li, F.: Spin excitations in $K_{0.84}Fe_{1.99}Se_2$ superconductor as studied by Mössbauer spectroscopy. Chin. Phys. B **21**, 047601 (2012)
6. Cai, Y., Wang, Z., Wang, Z.W., Sun, Z.A., Yang, H.X., Tian, H.F., Ma, C., Zhang, B., Li, J.Q.: Microstructural properties of $K_{0.8}Fe_{16}S_2$, $K_{0.8}Fe_{175}Se_{2-y}S_y$ ($0 \leq y \leq 2$) and $K_{0.8}Fe_{15+x}S_2$ ($0 < x \leq 0.5$) single crystals. Europhys. Lett. **103**, 37010 (2013)
7. Lei, H., Abeykoon, M., Bozin, E.S., Petrovic, C.: Spin-glass behavior of semiconducting $K_xFe_{2-y}S_2$. Phys. Rev. B **83**, 180503 (2011)
8. Ying, J.J., Xiang, Z.J., Li, Z.Y., Yan, Y.J., Zhang, M., Wang, A.F., Luo, X.G., Chen, X.H.: Physical properties of $A_xFe_{2-y}S_2$ (A = K, Rb, and Cs) single crystals. Phys. Rev. B **85**, 054506 (2012)
9. Ying, J.J., Wang, X.F., Luo, X.G., Wang, A.F., Zhang, M., Yan, Y.J., Xiang, Z.J., Liu, R.H., Cheng, P., Ye, G.J., Chen, X.H.: Superconductivity and magnetic properties of single crystals of $K_{0.75}Fe_{1.66}Se_2$ and $Cs_{0.81}Fe_{1.61}Se_2$. Phys. Rev. B **83**, 212502 (2011)
10. Wang, D.M., He, J.B., Xia, T.-L., Chen, G.F.: Effect of varying iron content on the transport properties of the potassium-intercalated iron selenide $K_xFe_{2-y}Se_2$. Phys. Rev. B **83**, 132502 (2011)
11. Ksenofontov, V., Wortmann, G., Medvedev, S.A., Tsurkan, V., Deisenhofer, J., Loidl, A., Felser, C.: Phase separation in superconducting and antiferromagnetic $Rb_{08}Fe_{16}Se_2$ probed by Mössbauer spectroscopy. Phys. Rev. B **84**, 180508 (2011)
12. Shylin, S.I., Ksenofontov, V., Sedlmaier, S.J., Clarke, S.J., Cassidy, S.J., Wortmann, G., Medvedev, S.A., Felser, C.: Intercalation effect on hyperfine parameters of Fe in FeSe superconductor with $T_c = 42$ K. Europhys. Lett. **109**, 67004 (2015)